Engineering yeast for high-level production of diterpenoid sclareol

Metabolic Engineering 75 (2023) 19–28

Contents lists available at ScienceDirect

Metabolic Engineering

journal homepage: www.elsevier.com/locate/meteng

Engineering yeast for high-level production of diterpenoid sclareol

Xuan Cao [a,b,c,f], Wei Yu [a,d], Yu Chen [e], Shan Yang [a,d], Zongbao K. Zhao [a,c], Jens Nielsen [e], Hongwei Luan [a,c], Yongjin J. Zhou [a,b,c,*]

[a] Division of Biotechnology, Dalian Institute of Chemical Physics, Chinese Academy of Sciences, Dalian, 116023, China
[b] CAS Key Laboratory of Separation Science for Analytical Chemistry, Dalian Institute of Chemical Physics, Chinese Academy of Sciences, Dalian, 116023, China
[c] Dalian Key Laboratory of Energy Biotechnology, Dalian Institute of Chemical Physics, Chinese Academy of Sciences, Dalian, 116023, China
[d] University of Chinese Academy of Sciences, Beijing, 100049, China
[e] Department of Biology and Biological Engineering, Chalmers University of Technology, SE-412 96, Gothenburg, Sweden
[f] Jinan Microecological Biomedicine Shandong Laboratory, Jinan, 250117, China

A B S T R A C T

The diterpenoid sclareol is an industrially important precursor for alternative sustainable supply of ambergris. However, its current production from plant extraction is neither economical nor environmental-friendly, since it requires laborious and cost-intensive purification procedures and plants cultivation is susceptible to environmental factors. Engineering cell factories for bio-manufacturing can enable sustainable production of natural products. However, stringent metabolic regulation poses challenges to rewire cellular metabolism for overproduction of compounds of interest. Here we used a modular approach to globally rewire the cellular metabolism for improving sclareol production to 11.4 g/L in budding yeast *Saccharomyces cerevisiae*, the highest reported diterpenoid titer in microbes. Metabolic flux analysis showed that modular balanced metabolism drove the metabolic flux toward the biosynthesis of targeted molecules, and transcriptomic analysis revealed that the expression of central metabolism genes was shaped for a new balanced metabolism, which laid a foundation in extensive metabolic engineering of other microbial species for sustainable bio-production.

1. Introduction

Sclareol, a diterpene alcohol, has been used for the synthesis of fragrance molecules Ambrox®, which were traditionally extracted from sperm whale, now an endangered species (Zerbe and Bohlmann, 2015). Currently, the main sources of sclareol are the flowers and leaves of *Salvia sclarea*, a biennial herb native of Southern Europe. However, the low concentration of diterpenoids in *planta* with complex mixtures, requires laborious and cost-intensive purification procedures and the susceptibility to environmental factors such as land use and climate, make it neither economical nor environmental-friendly. Alternatively, microbes are considered as ideal biocatalysts for biosynthesis of these precious molecules by introducing multiple-enzymatic cascade reactions (Chen et al., 2020; Nielsen and Keasling, 2016).

Previously studies have harnessed *Escherichia coli* (Schalk et al., 2012) and *Saccharomyces cerevisiae* (Trikka et al., 2015) for sclareol production by engineering the isoprenoid pathway and diterpenoid synthases. However, the biosynthesis efficiency remains to be largely improved (Trikka et al., 2015). In general, engineering heterologous biosynthetic pathways requires perturbation of endogenous cellular metabolism, which suffers from the stringent metabolic regulation (Nielsen and Keasling, 2016). Furthermore, construction of microbial cell factories from scratch is time consuming and labor intensive because it requires extensive rewiring of the native metabolic network toward product biosynthesis. Construction of a platform strain with sufficient supply of precursors and driving forces can facilitate the construction of efficient microbial cell factories, however, metabolic stress may ensue because of an imbalance in the metabolic network. These challenges severely hamper metabolic engineering endeavors and result in low performance of microbial cell factories (Wu et al., 2016).

Previous diterpenoid production focused mainly on engineering the isoprenoid biosynthetic pathway and the diterpenoid synthase by modular optimization of gene expression (Hu et al., 2020; Zhou et al., 2012; Zhou, 2018). The production of diterpenoids in yeast (<4 g/L) is always too low for commercial process (Guo et al., 2019; Hu et al., 2020; Zhou et al., 2012). These low productions might attribute to insufficient precursor acetyl-CoA because of metabolic rigidity (Gaspar and Csermely, 2012; Nielsen and Keasling, 2016; Stephanopoulos and Vallino, 1991). Alternatively, global rewiring of cellular metabolism could help to reach a new balanced metabolic pattern for overproduction of target products. In this study, we systematically engineered the metabolism of *S. cerevisiae* for improving the production of sclareol (11.4

* Corresponding author. Division of Biotechnology, Dalian Institute of Chemical Physics, Chinese Academy of Sciences, Dalian, 116023, China.
E-mail address: zhouyongjin@dicp.ac.cn (Y.J. Zhou).

https://doi.org/10.1016/j.ymben.2022.11.002
Received 1 June 2022; Received in revised form 1 November 2022; Accepted 8 November 2022
Available online 9 November 2022

g/L), the highest titers reported so far (Fig. 1). We found that engineering central metabolism boosted the biosynthetic efficiency, which can be easily applied for sustainable supply of sclareol.

2. Material and methods

2.1. Strains, media, and reagents

Escherichia coli strain DH5α was used for plasmid construction and amplification. The key and milestone strains in this study were listed in Table 1 and the whole *S. cerevisiae* strains and plasmids are listed in Tables S1 and S2. The flowchart of yeast strain construction is described in Fig. S1. *S. cerevisiae* cells were cultured at 30 °C in YPD medium (1% yeast extract, 2% peptone, and 2% glucose) or SD medium (0.67% yeast nitrogen base without amino acids, 2% glucose with histidine (20 mg/L) and/or uracil (20 mg/L) if needed. Agar (1.6% w/v) was added for preparing solid media for screening of transformants. For fermentations, a minimal medium was used that contained 2.5 g/L $(NH_4)_2SO_4$, 14.4 g/L KH_2PO_4, 0.5 g/L $MgSO_4{\cdot}7H_2O$, 20 g/L glucose, trace metals, and vitamin solutions (Verduyn et al., 1992) supplemented with 40 mg/L histidine and/or 60 mg/L uracil if needed. Phanta HS Super-Fidelity DNA Polymerase, Taq DNA polymerase and One Step Cloning Kit (plasmids construction) were purchased from Vazyme Biotech Co., Ltd. (Nanjing, China). DNA gel purification and plasmid extraction kits were purchased from Sangon Biotech Co., Ltd. (Shanghai, China). All chemicals including analytical standards were purchased from Sigma-Aldrich unless stated otherwise. All primers (Table S3) were synthesized from Sangon Biotech Co., Ltd and exsyn-bio Technology Co., Ltd. All codon optimized heterologous genes (Table S4) were synthesized by Genewiz.

2.2. Genetic manipulation

A *CAS9* expression cassette fused with *KanMX* (P_{TEF1}-*CAS9*-T_{CYC1}-*KanMX*) was amplified from plasmid pECAS9-kanMX-gRNA and integrated at the *XI-5* site (Mikkelsen et al., 2012) in wild type CEN. PK 113-11C. The strain with *KanMX* knocked out was named as XC01. All guide-RNAs (gRNAs) were designed by the CHOPCHOP webtool (http://chopchop.cbu.uib.no), and gRNA-expressing plasmids were constructed according to described methods (Mans et al., 2015; Yang et al., 2020). The donor DNAs for gene deletion and integration were assembled by one-pot fusion PCR. The *TPS* and *LPPS* genes were obtained from pSclareol-1 plasmid(Yang et al., 2013). The *TPS-LPPS* and *LPPS-TPS* fusions were assembled with a GGGS linker. The *TPS-LPPS*, *LPPS-TPS* and *TPS* + *LPPS* (P_{eTDH3}-*LPPS*-T_{PYK1}-T_{PRM9}-*TPS*-P_{eTDH3}-T_{pYX212}) fusions were cloned into pYX312 with EcoRI/HindIII digestion

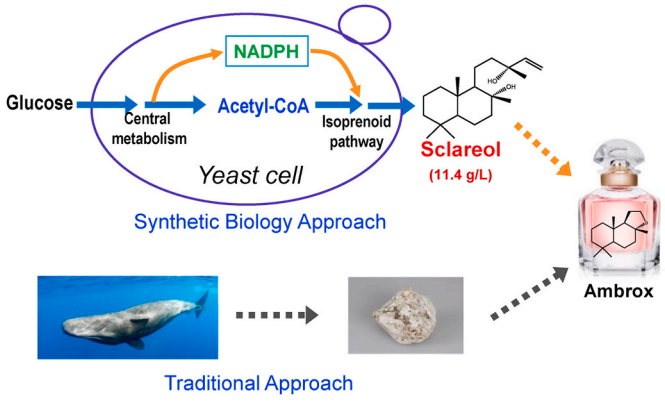

Fig. 1. Engineering yeast for sustainable production of sclareol, a precursor for synthetic of fragrance molecules Ambrox. Systematically engineering yeast cellular metabolism for enhancing supply of precursor acetyl-CoA and cofactor NADPH, and driving the metabolic flux of isoprenoid pathway, enabled overproduction of sclareol (11.4 g/L).

Table 1
Sclareol production of the key engineered *S. cerevisiae* strains.

Strain name	Metabolic engineering strategy	Titer (mg/L)
CEN.PK 113–11C	Wild-type	0
CXM01*	Integration of sclareol synthases	0.22
CXM17	Integration of sclareol synthases; Isoprenoid pathway optimization	293
CXM18	Integration of sclareol synthases; Isoprenoid pathway optimization; regulation factors engineering	584
SCX38	Integration of sclareol synthases; Central metabolism engineering; Isoprenoid pathway optimization	353
SCX42	Integration of sclareol synthases; Central metabolism engineering; Isoprenoid pathway optimization; regulation factors engineering	918
SCX42-LAC1-OYE3	Integration of sclareol synthases; Central metabolism engineering; Isoprenoid pathway optimization; regulation factors engineering, overexpressing *LAC1* and *OYE3*	1150

The strain information can be found in Supplementary Table 3.

to produce plasmids pYX312-TL, pYX312-LT, and pYX312-L + T. The promoter and open reading frame (ORF) of *ERG20* (from −532 bp to 1059 bp) was replaced with P_{TDH3} and mutated *ERG20**(*ERG20*^{F96C}). The SpHMGR gene from *Silicibacter pomeroyi* and the *MBP* gene from *E. coli* were codon-optimized for *S. cerevisiae*. The truncated *HMG1* gene (*tHMG1*, from 1588 bp to 3165 bp), *ERG10* gene, and *BTS1* gene were amplified from CEN. PK 113-11C genomic DNA. The mutated *HMG2K6R* gene (*HMG2**) was constructed by a target mutation PCR with CEN. PK 113-11C genomic DNA as a template.

2.3. Strain construction

The genome integrated gene expression cassettes were described in Fig. S2. Central metabolism engineering was based on strain Y&Z036, the modifications were as follows: *HIS3*, *'tesA* and *RtFAS1*, *RtFAS2* genes were deleted; The promoter of *ACC1* was switched from P_{TEF1} to P_{ACC1}; *FAA1* gene was in-situ restored. *FAA4* gene was in-situ restored with *tHMG1* integrated simultaneously; *POX1* gene was in-situ restored with *SpHMGR* integrated in the meantime. The isoprenoid pathway optimizations were as follows: the *MBP-TL* fusion genes were integrated in the *XI-3* site; the *HMG2** and *ERG10* genes were integrated in the *XII-2* site; the extra two copies of *HMG2** were integrated in the *XII-3* site; the *ERG9* promoter was replaced with P_{HXT1} or deleted from −220 to −175 bp. The fusion of *BTS1-PaGGPPS*, *BTS1-ERG20** and *ERG20-ERG20** were integrated in the *XI-2* site. The *tHMG1* and *SpHMGR* expressing cassettes were integrated in *XII-5* site in strain CXM21, CXM22, CXM17 and CXM18 with CENPK. 113-11C. The regulation factors *ROX1*, *DOS2*, *VBA5*, *YER134C*, *YNR063W* and *YGR259C* were seamlessly knocked out. Taking the example of the integration of *MBP-TL* fusion (P_{GAL7}-*MBP-TL*-T_{ADH1}) into the *XI-3* site in SCX22, the upstream homologous arm *XI-3up*, promoter P_{GAL7}, terminator T_{ADH1} and downstream homologous arm *XI-3dw* were amplified from CEN. PK 113-11C genome by using primer pair P030/031, P032/033, P038/039 and P040/041, respectively. The gene *MBP* was amplified from the codon optimized gene by using primer pair P034/P035 and TL fusion was amplified from the plasmid pYX312-TL by using primer pair P036/037. Then the fragments mentioned above were assembled by over-lap extension PCR, the obtained expression cassette was transformed along with pgRNA-XI-3 into SCX22 and selected on SD-URA-HIS (6.7 g/L YNB without amino acids, 20 mg/L histidine and 20 mg/L uracil and 20 g/L glucose and 15 g/L agar). Clones were verified by colony PCR. Subsequently, 3 clones with correct module integration were cultivated overnight in YPD liquid medium and then plated on SD+5-FOA plates after wash for looping out of *URA3*.

2.4. Batch and fed-batch fermentation

The batch fermentation was conducted in 100 mL shake flasks with 15 ml minimal medium consisting of 2.5 g/L $(NH_4)_2SO_4$, 14.4 g/L KH_2PO_4, 0.5 g/L $MgSO_4 \bullet 7H_2O$, 20 g/L glucose, trace metal and vitamin solutions. The yeast cells were cultivated at 30 °C, 220 rpm for 4 days (Zhichu Shaker ZQZY-CS8) with initial inoculation OD_{600} of 0.2.

The fed-batch fermentations for sclareol production were performed in 0.25 L shake flasks or 1.0 L bioreactors. The fed-batch in shake flasks were conducted with an initial working volume of 50 mL minimal medium and an initial inoculation OD_{600} of 0.2. The temperature was set as 30 °C, and agitation speed was set as 220 rpm. The pH was adjusted to 5.6 by addition of 4 M KOH once a day. During the fed-batch cultivation, the cells were fed with 1–2 mL medium A or B when glucose was depleted. Medium A contained 500 g/L glucose solution, 15 g/L $(NH_4)_2SO_4$, 9 g/L KH_2PO_4, 1.5 g/L $MgSO_4 \bullet 7H_2O$, 3 × trace metal and 3 × vitamin solutions, Medium B contained 500 g/L glucose solution, 7.5 g/L $(NH_4)_2SO_4$, 43.2 g/L KH_2PO_4, 1.5 g/L $MgSO_4 \bullet 7H_2O$, 3 × trace metal and 3 × vitamin solutions. The fed-batch fermentation in bioreactors was conducted with an initial working volume of 0.4 L by using a DasGip Parallel Bioreactors System (DasGip). The batch fermentation was conducted in a minimal medium consisting of 2.5 g/L $(NH_4)_2SO_4$, 14.4 g/L KH_2PO_4, 0.5 g/L $MgSO_4 \bullet 7H_2O$, 20 g/L glucose, trace metal and vitamin solutions. The initial inoculation OD_{600} was 0.4. The temperature was set as 30 °C, initial agitation speed was set as 800 rpm and increased to maximally 1200 rpm depending on the dissolved oxygen (DO) level. Aeration was initially set 36 sL/h and increased to maximally 48 sL/h depending on the DO level. The DO level was maintained above 30%, and the pH was kept 5.6 by automatic addition of 4 M KOH and 2 M HCl. During the fed-batch cultivation, the cells were fed with a medium (500 g/L glucose solution, 10 g/L $(NH_4)_2SO_4$, 57.6 g/L KH_2PO_4, 2 g/L $MgSO_4 \bullet 7H_2O$, 4 × trace metal and 4 × vitamin solutions) at a feeding rate that was exponentially increased ($\mu = 0.05\ h^{-1}$) to maintain a constant biomass-specific glucose consumption rate. The initial feeding rate was calculated using the biomass yield and concentration that were obtained during prior duplicate batch cultivations with these strains. The feeding was started once glucose was depleted. When the residual glucose existed, the feeding was stopped. After fermentation, all particles were re-suspended to the liquid culture for quantification of the total sclareol titers. Measurements were performed in triplicates.

2.5. Product extraction and quantification

Sclareol was extracted by hexane containing 40 mg/L sclareolide as an internal standard. Cell cultures should be condensed or diluted depending on the titer of sclareol. In brief, when sclareol titer was less than 20 mg/L, the 2 mL hexane was added to 4 mL cell culture and the mixtures were shaken for 30 min at 1400 rpm by using a vortex mixer, and then centrifuged at 1000×*g* to promote phase separation. Then, 1 mL of the upper organic phase was evaporated for 45 min to dryness. Next, the extracted sclareol was resuspended in 100 μL hexane without sclareolide; when sclareol titer was between 20 and 100 mg/L, the hexane and cell culture should be mixed at a proportion of 1:1. After being vortexed and centrifuged, the upper hexane was taken for product analysis; when sclareol titer was more than 100 mg/L, the cell culture was diluted by 10 or 20-fold. Sclareol was quantified by Gas Chromatography-Mass Spectrometer (GC-MS, ThermoFisher Scientific) equipped with a Zebron ZB-5MS GUARDIAN capillary column (30 m × 0.25 mm x 0.25 mm, Phenomenex) and a DSQII mass spectrometer (ThermoFisher Scientific). The GC program was as follows: initial temperature of 150 °C, hold for 1 min; ramp to 220 °C at a rate of 20 °C/min, hold for 1 min; then raised to 300 °C at a rate of 20 °C/min and hold for 2 min. The temperature of inlet, mass transfer line and ion source were kept at 250, 300 and 230 °C, respectively. The injection volume was 1 μL. The flow rate of the carrier gas (helium) was set to 1.0 mL/min, and data were acquired at full-scan mode (50–650 m/z). Final quantification was performed using the Xcalibur software.

2.6. Quantification of NADP(H) and acetyl-CoA

For $NADP^+$ and NADPH assay, 10 mL cell culture was centrifuged at 3000×*g* for 5 min, and the cell pellet was washed twice with 10 mM PBS. Then the cell was suspended in 300 μL 0.2M HCl (for $NADP^+$ assay) or 0.2 M NaOH (for NADPH assay) and disrupted the cell sonication for 30 min. The cell solution was heated in 60 °C for 30 min, then neutralized with 300 μL 0.2M NaOH 0.2 M HCl respectively. The solution was centrifuged at 13,000×*g* for 5 min and supernatant was subjected to $NADP^+$ or NADPH assay. The assay was performed by using a reagent mixture consisting of equal volumes of 1.0 M bicine buffer (pH 8.0), 30 mM glucose-6-phosphate, 40 mM EDTA (pH 8.0), 4.2 mM 3-(4,5-dimethyl-2-thiazolyl)-2,5-diphenyl-2H-tetrazolium bromide, two volumes of 16.6 mM phenazine ethosulfate and three volumes of distilled water. 10 μL neutralized extract and 180 μL reagent mixture were added to 96-well plates and 10 μL glucose-6-phosphate dehydrogenase (100 U/mL) was added to start the assay. The absorbance at 570 nm was recorded for 10 min (every 20 s for a record) at 25 °C. The assay was calibrated with 0.01–0.05 mM standard solutions of $NADP^+$ or NADPH and the slope was correlated to the concentrations of cofactor concentration in the extracts from each sample by a linear fit equation.

For cellular acetyl-CoA assay, 2 mL cell culture was centrifuged at 3000×*g* for 5 min, and the cell pellet was washed twice with 10 mM PBS. Then the cell was suspended in 500 μL PBS and disrupted with cell sonication for 30 min. The cell solution was subjected to acetyl-CoA assay, by using Acetyl-CoA ELISA Kit (No. D751001, Sangon Biotech, Shanghai, China).

2.7. Metabolic flux analysis

The latest genome-scale metabolic model of *S. cerevisiae* Yeast8(Lu et al., 2019) was extended by adding heterologous pathways, which was subsequently used to generate strain-specific models for strains CXM18 and SCX42 by blocking corresponding reactions. To simulate flux distributions, flux balance analysis was performed using various strain-specific models constrained by experimentally measured glucose uptake, ethanol production, sclareol production, and growth rates (Table S6) with the objective function of ATP maintenance maximization. Model construction and simulations were performed in MATLAB with the COBRA toolbox(Heirendt et al., 2019).

2.8. Transcriptome analysis

CXM01*, CXM17, CXM18, SCX38, and SCX42 were cultivated in minimal medium at 30 °C, 220 rpm. Cells were collected in the glucose-consumed phase when the glucose concentration remained about 10 g/L and in the ethanol consumed phase when the glucose was depleted. Cells were stored at −80 °C before RNA extraction. Total RNA was extracted with the RNeasy Mini Kit (Qiagen, Hilden, Germany) according to the manufacturer's instructions. The quality of RNA samples was assessed with the RNA Nano 6000 Assay Kit of the Bioanalyzer 2100 system (Agilent Technologies, CA, USA). The clustering of the index-coded samples was performed on a cBot Cluster Generation System using TruSeq PE Cluster Kit v3-cBot-HS (Illumia) according to the manufacturer's instructions. After cluster generation, the library preparations were sequenced on an Illumina Novaseq platform at Novogene Bioinformatics Technology Co. Ltd. Reference genome and gene model annotation files were downloaded from the genome website. We selected Hisat2 as the mapping tool. FeatureCounts v1.5.0-p3 was used to count the reads numbers mapped to each gene. Differential expression analysis of two conditions/groups (three biological replicates per condition) was performed using the DESeq2 R package (1.20.0). Genes with an adjusted P-value <0.05 found by DESeq2 were assigned as differentially expressed. Gene Ontology (GO) enrichment analysis of

differentially expressed genes was implemented by the clusterProfiler R package, in which gene length bias was corrected.

3. Results

3.1. Engineering sclareol synthase

Sclareol biosynthesis is catalyzed by class I and class II diterpene synthases Tps and Lpps from *Salvia sclarea* via a two-step enzymatic reaction (Schalk et al., 2012). To favor substrate channeling between Lpps and Tps, we genetically fused the two synthases. We found that the Tps-Lpps (TL) fusion improved sclareol biosynthesis by 6.7-fold compared with separate enzymes; the Lpps-Tps fusion had a more moderate improvement (Fig. 2). This observation was similar to other studies on engineering diterpene synthases for miltiradiene synthesis in yeast (Hu et al., 2020; Zhou et al., 2012). We also joined a maltose-binding protein (MBP) moiety to the N-terminus of Tps-Lpps (*MBP-TL*) for improving the enzymatic stability (Reider Apel et al., 2017); this modification improved sclareol production by 43% (strain SCX23 in Fig. 2). For stable expression, we integrated the *MBP-TL*-expressing cassette into *XI-3* site of the yeast genome (Mikkelsen et al., 2012).

3.2. Metabolic rewiring for sclareol biosynthesis

We then tried to enhance sclareol production by systematically engineering the cellular metabolism. To facilitate the modular metabolic engineering, we divided the global metabolism into three modules: central metabolism for supply of acetyl-CoA, isoprenoid biosynthesis pathways and regulation factor modules (Fig. 3A).

We firstly overexpressed $ERG20^{F96C}$ for supply of geranylgeranyl diphosphate (GGPP) (Ignea et al., 2015), *tHMG1* (Polakowski et al., 1998) and *SpHMGR* (Meadows et al., 2016) for biosynthesis 3-hydroxy-3-methylglutaryl-coenzyme A (HMG-CoA). The resulting strain CXM21 had a slightly higher sclareol production (1.03 mg/L) compared with the control strain CXM01* (0.91 mg/L) (Fig. 3C). Further overexpression of the *ERG10* gene encoding acetoacetyl-CoA thiolase, and *HMG2** ($HMG2^{K6R}$) encoding a mutant of endogenous Hmgr (Ignea et al., 2012), improved sclareol production to 2.20 mg/L (strain CXM22). Although these modifications improved the biosynthesis of sclareol, its titer was still low. We assumed that the limited supply of precursor acetyl-CoA and cofactor NADPH might be a bottleneck that neutralized the enhancing isoprenoid pathway. It was easy to come up with the idea to further rewire the central metabolism for enhancing the supply of acetyl-CoA and NADPH as we did previously for overproduction of free fatty acids (FFA) (Yu et al., 2018; Zhou et al., 2016). However, copying these metabolic engineering strategies requires manipulation of 18 genes that are involved in acetyl-CoA biosynthesis and NADPH supply. To avoid tedious genetic engineering, we explored

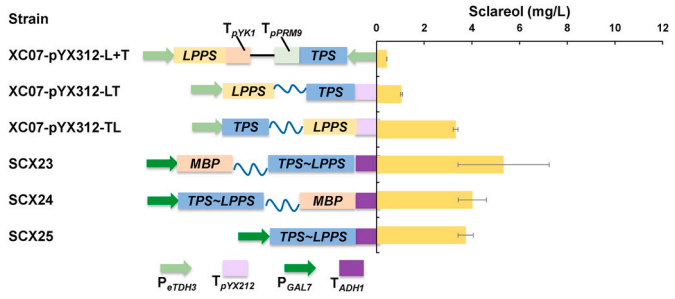

Fig. 2. Engineering diterpenoid synthase for improved sclareol production. The *LPPS* and *TPS* genes were expressed in three ways in strain XC07. Then, the *TPS-LPPS* fusion was fused with *MBP* in strain SCX22. The linker was GGGGS. All data represent the means ± s.d. of three yeast clones.

the possibility to transform the cellular metabolism from FFA biosynthesis to diterpenoid production by taking full advantage of this excellent chassis with rewired central metabolism (Fig. 3B). This kind of transform can save time of 18 genes' manipulation (Fig. S3) and can also be easily adapted for construction of versatile cell factories from a chassis strain. Simply *in situ* recovery of the deleted *FFA1/4* and removal of the overexpressed genes (*FAS1/2 and TESA*) for fatty acid biosynthesis (Fig. 3B), created a chassis strain with efficient supply of acetyl-CoA and NADPH. Overexpressing *tHMG1*, *SpHMGR,* and *ERG20** in this chassis resulted in a 6.4 mg/L production of sclareol (strain SCX23), which was 5.2 times higher than the control strain CXM21, and further overexpression of *ERG10* and *HMG2** resulted in a 22-fold improvement (49.1 mg/L in strain SCX28) compared with strain CXM22 (Fig. 3C). The improvement of isoprenoid biosynthesis engineering in the chassis with enhanced central metabolism was more significant compared with that in wild-type background (Fig. 3C). This observation demonstrated that the sufficient supply of acetyl-CoA and NADPH released the potential of enhanced isoprenoid biosynthesis by driving the metabolic flux toward isoprenoid pathway. We also observed that SCX23-β, with expression of only sclareol synthase in the engineered central metabolism background, had retarded growth, while growth of strain SCX23 and SCX28 was restored (Fig. 3C), which might be attributed to imbalanced metabolic flux. Because the rewired central metabolism caused acetyl-CoA and NADPH accumulating without a strong output (Fig. 3D), while an enhanced isoprenoid pathway pulled extra acetyl-CoA and NADPH to sclareol biosynthesis and relieve the perturbation to cell growth (Fig. 3E and F).

With this efficient chassis, we next comprehensively engineered the isoprenoid pathway to improve sclareol biosynthesis. Expressing two extra copies of *HMG2** genes improved sclareol production to 120.3 mg/L in strain SCX32 (Fig. 3G). Down-regulation of *ERG9*, by replacing its native promoter with the *HXT1* promoter (Xie et al., 2015), improved sclareol production to 310.5 mg/L by blocking ergosterol biosynthesis. We also tried to introduce a GGPP synthase (GGPPS) from *Phomopsis amygdali* that catalyzes GGPP formation directly from the C5 units of IPP (isopentenyl diphosphate) and DMAPP (dimethylallyl diphosphate) (Callari et al., 2018). Overexpressing the gene fusion *BTS1-PaGGPPS* improved sclareol production to 347.4 mg/L in strain SCX38 (Fig. 3G and Table 1). It has been shown that engineering the regulation factors improved production of isoprenoids (Trikka et al., 2015). Thus, we deleted regulator genes *ROX1*, *DOS2*, *VBA5*, *YER134C*, *YNR063W*, and *YGR259C* in strain SCX38 and observed a 1.7-fold improvement of sclareol production in SCX42 to 918 mg/L (Fig. 3G and Table 1). Culturing SCX42 in nutritious YPD media obtained 1.83 g/L of sclareol production (Fig. 3H and Fig. S4).

3.3. Metabolic profiling of engineered strains

We profiled the engineered strains to show the effect of each module on sclareol biosynthesis (Figs. 3A and 4A). In a wild-type background, optimization of the isoprenoid pathway produced a specific sclareol titer of 13.4 mg/L/OD_{600} (strain CXM17), and further engineering regulatory factors improved sclareol production by 2.6-fold (35.0 mg/L/OD_{600} in strain CXM18). Yet, on the basis of engineered central metabolism, optimizing isoprenoid pathway (SCX38) and plus regulatory factors (SCX42) led to about 2-fold higher sclareol production, compared to CXM17 and CXM18, respectively, whereas there was a marginal improvement when only sclareol synthases were expressed (SCX23-β vs CXM01*) (Fig. 4A). These data showed that there was a synergic effect of the three modules for providing an efficient metabolic channel toward sclareol biosynthesis.

We next conducted the metabolic flux analysis of SCX42 and the control stain CXM18 by using physiological parameters from a batch fermentation (Table S2), which showed that globally rewired central metabolism had higher metabolic flux toward acetyl-CoA biosynthesis as well as pentose phosphate pathway (PPP) for NADPH regeneration

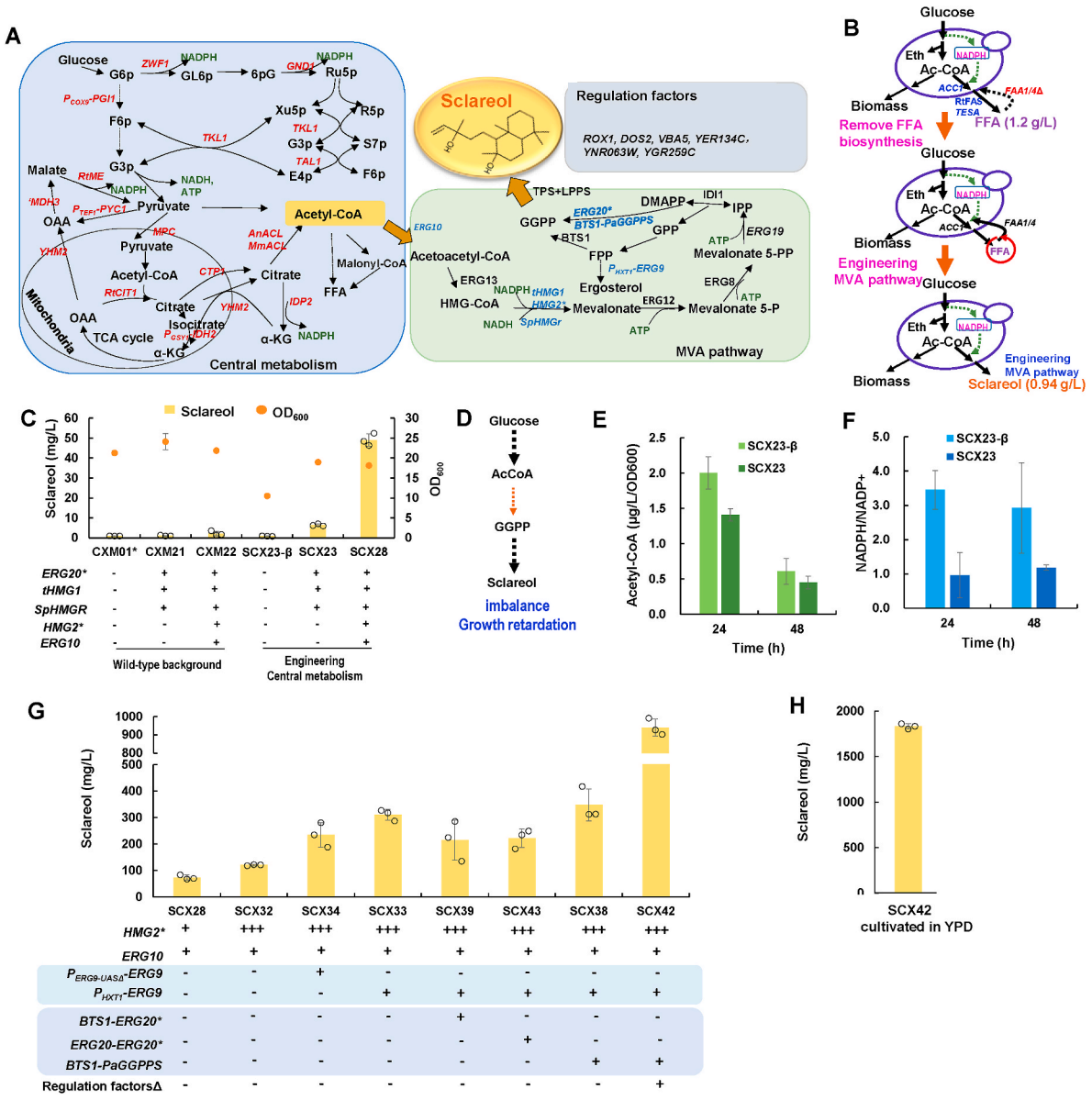

Fig. 3. Global metabolic rewiring of yeast metabolism for production of sclareol. (A) Global and modular optimization of central metabolism and the isoprenoid pathway for production of sclareol with enhanced the supply of precursor acetyl-CoA and cofactor NADPH. Modules 1–3 in different colors represent central metabolism, the isoprenoid pathway, and regulation factors, respectively. The detailed gene annotations were shown in Table S5 (B) The procedure of the metabolic transforming of a FFA-overproducing yeast to a sclareol producing yeast. The partial modifications of FFA biosynthesis pathway was restored. The isoprenoid pathway engineering was conducted simultaneously with reducing FFA biosynthesis. (C) Comparing the overexpressing key genes of isoprenoid pathway for sclareol production between the genetic backgrounds of wild-type and rewired central metabolism. (D) Schematic illustration of the metabolic imbalance of strain SCX23-β with enhanced central metabolism and overexpressed sclareol synthase, which retarded cell growth. (E)The acetyl-CoA level in SCX23-β and SCX23 at 24 and 48 h. (F) The NADPH/NADP$^+$ level in SCX23-β and SCX23 at 24 and 48 h. (G) Systematic optimization of isoprenoid pathway and deletion of the downregulating genes for sclareol production in a background strain with rewired central metabolism. The cells were cultivated in minimal medium with 20 g/L glucose for 96 h. (H) SCX42 was cultivated in YPD medium for 6 days. All data represent the means ± s.d. of three yeast clones.

(Fig. 4B). In particular, the alternative citrate-lyase based acetyl-CoA biosynthesis pulled higher metabolic flux of tricarboxylic acid (TCA) cycle toward acetyl-CoA supply in strain SCX42. Even with enhanced isoprenoid biosynthetic pathway, engineered central metabolism drove two-fold higher high flux toward the biosynthesis of GGPP, the sclareol precursor (Fig. 4B). Consistently, of SCX42 had significantly higher sclareol production than CXM18 under fed-batch fermentation in shake flasks (Fig. S5), which demonstrated that metabolic rewiring indeed had a positive effect on sclareol biosynthesis.

3.4. Transcriptional analysis of the engineered strains

To further explore the metabolic regulation, we conducted transcriptional analysis of strain CXM01*, CXM17, CXM18, SCX38, and SCX42 of glucose consumption phase and ethanol consumption phase, respectively, because the partial engineered genes expressed responding to glucose concentration. At the end of glucose consumption phase, 3.4%, 41.3%, and 51.3% of the total genes were differentially expressed (padj <0.05) in strains CXM17, SCX38 and SCX42, compared with the

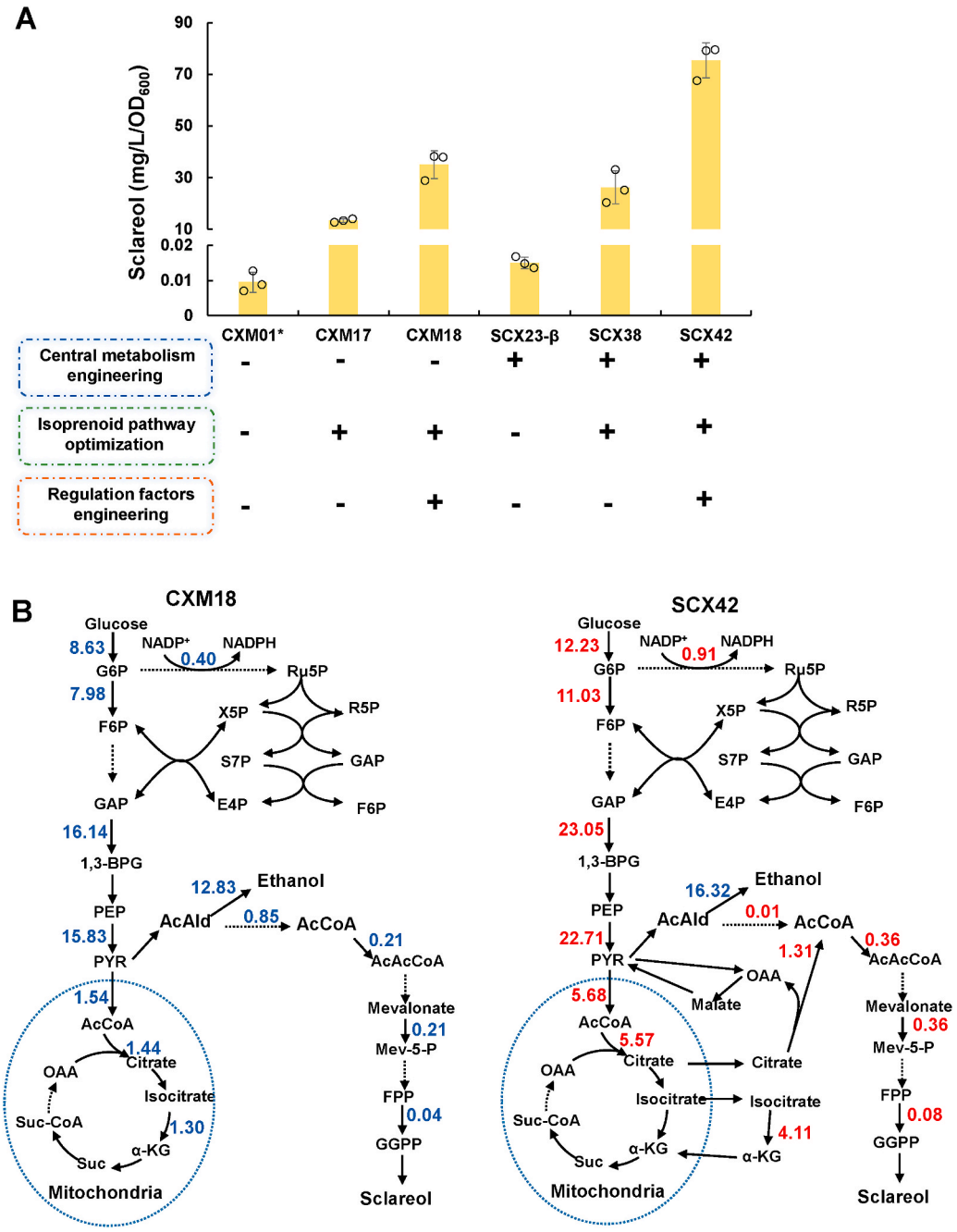

Fig. 4. Profiling the engineered strains with combined metabolic modules.
(A) The specific titer of sclareol. (B) Predicated metabolic flux distributions via flux balance analysis in CXM18 (left, without rewiring central metabolism strategy) and SCX42 (right, with rewired central metabolism). The metabolic flux was calculated based on the physiological parameters from a batch fermentation (Table S6).

control strain CXM01* (Fig. S6A). When ethanol was consumed, there were 5.0%, 58.1% and 41.1% of all genes differentially expressed in strains CXM17, SCX38 and SCX42 compared with the control strain CXM01* (Fig. S6B). These data indicated that optimization of isoprenoid pathway had a subtle effect on the overall metabolic network, whereas engineering central metabolism and regulation factors resulted in a global rewiring of cellular metabolism. The genes of glycolysis and TCA cycle were almost expressed invariably except that few genes involved in acetyl-CoA formation from pyruvate were up-regulated, and the genes of the PPP and isoprenoid pathway were partially up-regulated in strain CXM17 compared with CXM01* (Fig. 5A and Figs. S7 and S8). Although most of the genes in PPP and isoprenoid pathways exhibited up-regulation too, the gene expression profile was different between SCX38/SCX42 and CXM17 (Fig. 5A and Figs. S7 and S8). For example, *TKL2*, encoding transketolase 2, was up-regulated in CXM17, whereas it was down-regulated in SCX38/SCX42 with an overexpressed homology *TKL1*. *SOL4* (encoding 6-phosphogluconolactonase) and *GND2* (encoding 6-phosphogluconate dehydrogenase) of PPP pathway, were up-regulated in CXM17, but down-regulated in SCX38/SCX42 that contained genetically overexpressed *ZWF1* (encoding glucose-6-phosphate dehydrogenase) and *GND1* (Fig. 5A). These results suggested that cellular metabolism self-adapted in response to extensive metabolic perturbation. Strains SCX42 and SCX38 had similarly regulated gene expression profiles in the glucose consumption phase, whereas gluconeogenesis was up-regulated in SCX42 compared with SCX38 in the ethanol consumption phase. These results suggested that high sclareol

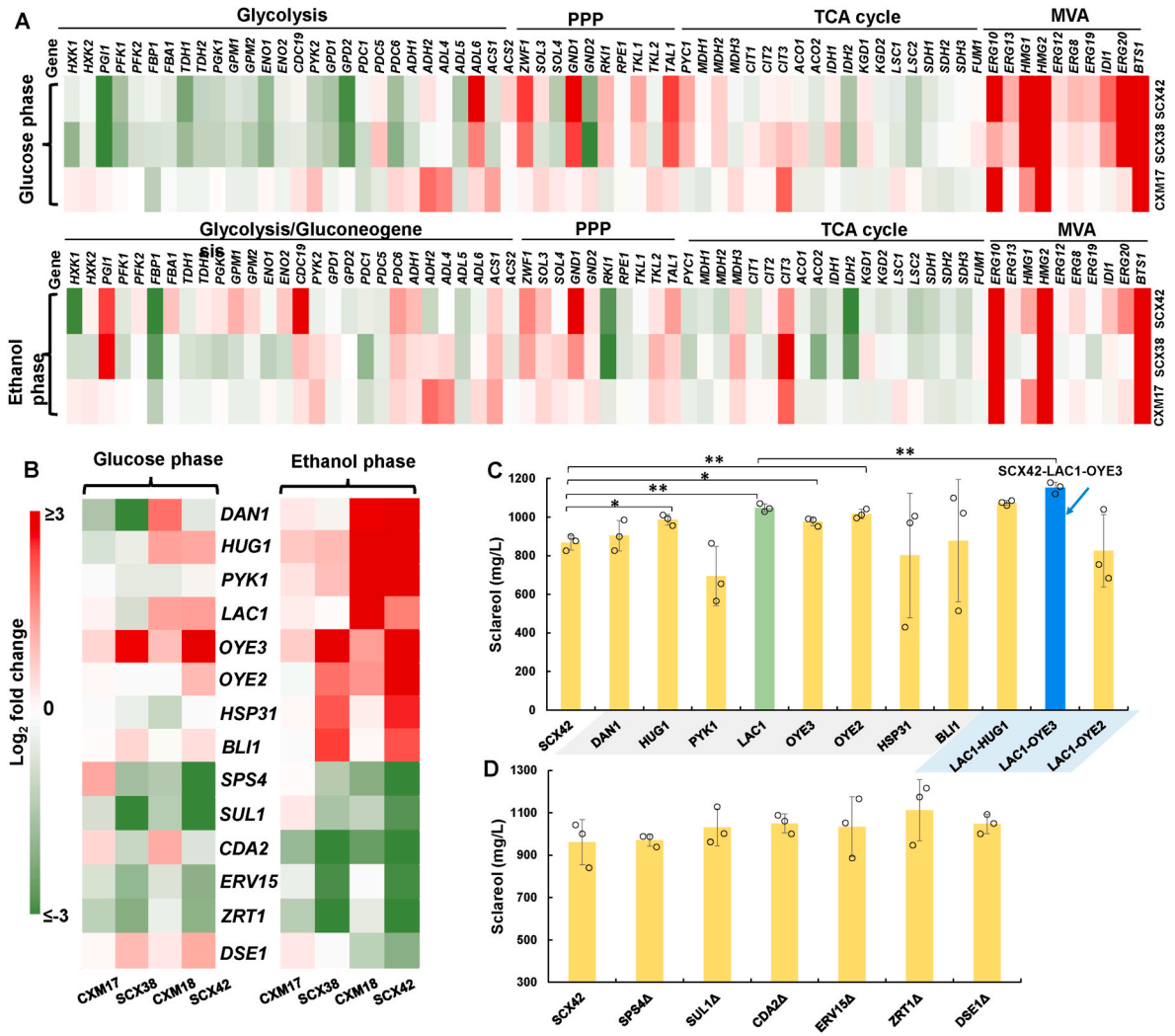

Fig. 5. Transcriptional analysis of the engineered strains. (A) Transcriptional levels of genes related to central metabolism and the isoprenoid pathway in CXM17, SCX38, and SCX42 compared with CXM01*. *HXK1/2*, hexokinase gene; *PGI1*, encoding phosphoglucose isomerase; *PFK1/2*, encoding phosphofructokinase 1 and 2; *FBP1*, fructose-1,6-bisphosphatase gene; *FBA1*, encoding fructose-bisphosphate aldolase; *TDH1/2*, encoding glyceraldehyde-3-phosphate dehydrogenase 1 and 2; *PGK1*, phosphoglycerate kinase gene; *GPM1/2*, encoding phosphoglycerate mutase 1 and 2; *ENO1/2*, encoding enolase 1 and 2; *CDC19*, encoding pyruvate kinase 1; *PYK2*, encoding pyruvate kinase 2; *GPD1/2*, encoding glycerol-3-phosphate dehydrogenase 1 and 2; *PDC1/5/6*, encoding pyruvate decarboxylase 1, 5 and 6; *ADH1/2*, alcohol dehydrogenase 1 and 2; *ALD4/5/6*, encoding aldehyde dehydrogenase 4, 5 and 6; *ACS1/2*, encoding acetyl coenzyme A (CoA) synthetase 1 and 2; *ZWF1*, encoding glucose-6-phosphate dehydrogenase; *SOL3/4*, encoding 6-phosphogluconolactonase 3 and 4; *GND1/2*, encoding 6-phophogluconate dehydrogenase 1 and 2; *RKI1*, encoding ribose-5-phosphate ketol-isomerase; *RPE1*, ribulose-5-phosphate epimerase gene; *TKL1/2*, encoding transketolase 1 and 2; *TAL1*, transaldolase gene; *MDH1/2/3*, encoding malate dehydrogenase 1, 2 and 3; *CIT1/2/3*, encoding citrate synthase 1, 2 and 3; *ACO1/2*, encoding aconitase 1 and 2; *IDH1/2*, encoding isocitrate dehydrogenase 1 and 2; *KGD1/2*, encoding α-ketoglutarate dehydrogenase 1 and 2; *LSC1/2*, encoding succinyl-CoA ligase 1 and 2; *SDH1/3*, encoding succinate dehydrogenase 1 and 3; *FUM1*, fumarase gene; *ERG10*, encoding acetoacetyl-CoA thiolase; *ERG13*, encoding HMG-CoA synthase;*HMG1/2*, encoding HMG-CoA reductase 1 and 2; *ERG8*,phosphomevalonate kinase gene; *ERG12*, mevalonate kinase gene; *ERG19*, encoding mevalonate diphosphate decarboxylase; *IDI1*, encoding isopentenyl diphosphate isomerase; *ERG20*, encoding FPP synthase; *BTS1*, encoding GGPP synthase. (B) Significantly regulated genes beyond central metabolism in CXM17, CXM18, SCX38 and SCX42 compared with CXM01*. *DAN1,* encoding cell wall protein*; HUG1,* encoding MEC1-mediated checkpoint protein; *PYK1*, encoding pyruvate kinase 1; *LAC1*, encoding sphingosine N-acyltransferase; *OYE3*, encoding NADPH dehydrogenase 3; *OYE2,* encoding NADPH dehydrogenase 2; *HSP31*, encoding glutathione-independent glyoxalase; *BLI1,* encoding biogenesis of lysosome-related organelles complex 1 subunit; *SPS4*, encoding sporulation-specific protein 4; *SUL1*, encoding sulfate permease 1; *CDA2*, encoding chitin deacetylase 2; *ERV15*, encoding ER-derived vesicles protein; *ZRT1,* encoding Zinc-regulated transporter 1; *DSE1,* encoding daughter-specific expression protein 1. (C) Overexpression of the up-regulated genes in strain SCX42 for sclareol production. (D) Deletion of the down-regulated genes in strain SCX42 for sclareol production. The cells were cultivated in minimal medium with 20 g/L glucose for 120 h. All data represent the means ± s.d. of three yeast clones. Significant difference of engineered strains from the parental strain is verified by Student's *t*-test (**p < 0.01, *p < 0.05).

production required a sufficient NADPH supply from up-regulated gluconeogenesis and PPP pathway. Overall, the extensive self-adjustment of gene expression in SCX42 suggested that flexibility of cellular metabolism could be stimulated by global metabolic rewiring, which was beneficial for reaching a new metabolic pattern such as sclareol overproduction.

In addition, there were some genes beyond the engineering targets that were differentially regulated (Fig. 5B), which might be helpful for sclareol biosynthesis. Thus, we sieved out a few of mutual or remarkably expressed genes by the differential expression analysis of SCX42 vs CXM18, SCX38 vs CXM17, SCX42 vs SCX38 and CXM18 vs CXM17 (Fig. 5B). We overexpressed the up-regulated genes by integrating one copy into genome, and knocked out the down-regulated target genes. Overexpression of *HUG1, LAC1*, *OYE2,* and *OYE3*, and disruption of

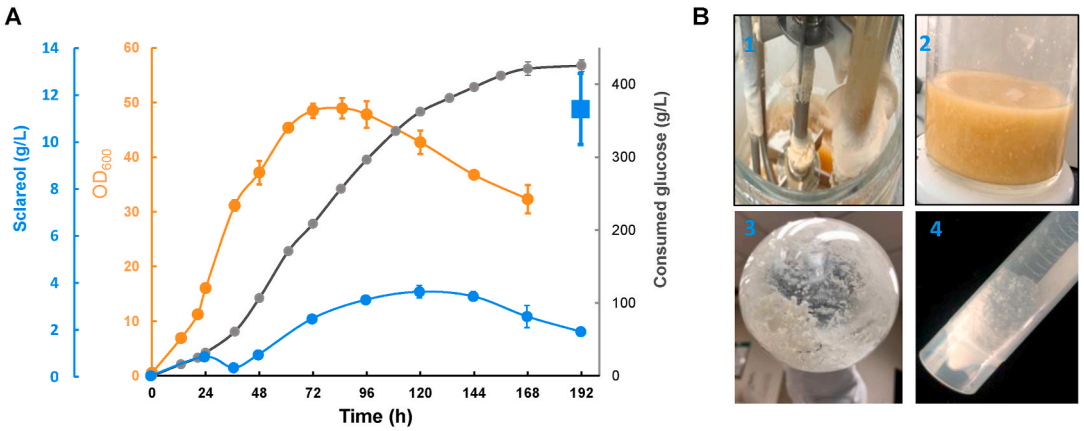

Fig. 6. Fed-batch fermentation of sclareol-producing strains. (A) Fed-batch fermentation of strain SCX42-*OYE3-LAC1*-UH under glucose-limited condition. Time courses of sclareol titers (blue circles) and final total titer (blue square) are shown. Since sclareol precipitated and adhered to the fermenter inner wall during fed-batch fermentation, the final overall titer (blue square) was quantified by taking precipitates into account. All data represent the means ± s.d. of two yeast clones. (B) High concentration of sclareol resulted in precipitation and sticked to the bioreactor. At the end of cultivation, the precipitates were resuspended in liquid for quantification and extracted by hexane, the sclareol powder was obtained by rotary evaporation.

SUL1, *CDA2*, *ERV15*, *ZRT1,* and *DSE1* improved sclareol production (Fig. 5C and D). Moreover, combinatorial overexpression of *LAC1* with *OYE3* further improved sclareol production by 20% (1.15 g/L). *HUG1*, encoding a MEC1-mediated checkpoint protein, was found to be involved in the control of nucleotide metabolism and was considered a regulator for fine-tuning of the ribonucleotide reductase activity (Meurisse et al., 2014). *LAC1*, encoding a sphingosine N-acyltransferase, has a homolog *LAG1* that has an important function in longevity (Megyeri et al., 2019). *OYE3* and *OYE2,* encoding NADPH dehydrogenases, had modulating functions in yeast oxidative stress and programmed cell death in yeast (Odat et al., 2007). These results showed that the higher production of sclareol resulted in self-regulation of some unassociated metabolic networks such as nucleotide metabolism, longevity, and cofactor regulation. We concluded that some hidden genes other than central metabolism respond to external metabolic rewiring, which is helpful for enhancing product biosynthesis.

3.5. Fed-batch fermentation for sclareol production

To evaluate the production potential, we conducted the fed-batch fermentation in shake flasks and bioreactors. To avoid supplementation of histidine and uracil, we constructed prototrophic strains by complementing the auxotrophic markers *URA3* and *HIS3*. We first optimized the feeding media in shake flasks (Fig. S9). Fed-batch fermentation of the best strain SCX42-*LAC1*-*OYE3*-UH resulted in overproduction of sclareol at 11.4 g/L (Fig. 6A), so-far the highest diterpenoid titer reported in the literature (Table 2). Interestingly, the high titer of sclareol formed a precipitate to stick on the bioreactor inner wall and the electrodes (Fig. 6B). Sclareol powder was obtained by extraction of hexane and further rotary evaporation. The purity of sclareol powder was almost the same as the sclareol standard (Fig. S10).

4. Discussion

Construction of efficient cell factories is challenging because of the complexity of cellular metabolism (Nielsen and Keasling, 2016). By

Table 2
Diterpenoid production in engineered microbes.

Diterpenoid	Host	Engineering strategy	Cultivation condition	Titer (g/L)	Productivity (g/L/h)	Yield (% theoretical yield)	Ref.
13R-manoyl oxide	*S. cerevisiae*	Isoprenoid pathway engineering	YPD, Glucose fed-batch	3	0.025	N.C.	Zhang et al. (2019)
Geranylgeraniol	*S. cerevisiae*	Isoprenoid pathway engineering	SMM, Glucose and ethanol fed-batch,	3.3	0.016	1.2	Tokuhiro et al. (2009)
Miltiradiene	*S. cerevisiae*	Engineering Isoprenoid pathway and diterpenoid synthase	SMM, Galactose fed-batch	3.5	0.017	9.2	Hu et al. (2020)
Taxadiene	*S. cerevisiae*	Engineering Isoprenoid pathway and diterpenoid synthase	YPG, batch, bioreactor	0.13	0.00066	N.C.	Nowrouzi et al. (2020)
Ent-kaurene	*Rhodosporidium toruloides*	Engineering GGPP synthase and diterpenoid synthase	Lignocellulosic hydrolysates, bioreactor	1.44	0.0051	N.C.	Geiselman et al. (2020)
Taxadiene	*E. coli*	Optimizing methylerythritol-phosphate (MEP) pathway	SMM, glycerol fed-batch	1.02	0.0085	N.C .	Ajikumar et al. (2010)
levopimaradiene	*E. coli*	Engineering MEP pathway and diterpenoid synthase	SMM, glycerol fed-batch	0.80	0.0048	N.C .	Leonard et al. (2010)
Sclareol	*E. coli*	Engineering MEP pathway	SMM, glycerol fed-batch	1.5	0.036	N.C.	Schalk et al. (2012)
Sclareol	*S. cerevisiae*	Engineering Isoprenoid pathway and regulation factors	SMM, shake flask, dodecane overlay	0.75	0.010	10.2	Trikka et al. (2015)
Sclareol	*S. cerevisiae*	Global metabolic rewiring	MM, Glucose fed-batch	**11.4**	**0.059**	**10.9**	**This study**

[a]MM, minimal media; SMM, semi-minimal media containing complex media component such as yeast extract; YPD, complex media containing 20 g/L peptone, 10 g/L yeast extract and 20 g/L glucose; YPG, complex media containing 20 g/L peptone, 10 g/L yeast extract and 20 g/L glactose.
[b] N.C., not calculated due to the lack of glucose consumption data or containing complex media component such as yeast extract.

comprehensively rewiring cellular metabolism in a modular manner, we successfully constructed versatile yeast cell factories for high-level production of sclareol (11.4 g/L), the highest titers yet reported in engineered microbes (Tables 1 and 2).

We previously comprehensively engineered the yeast cellular metabolism to reach a new harmonious metabolic pattern for production of an endogenous primary metabolite FFA (Yu et al., 2018). However, it is more challenging in engineering cell factories for production of exogenous metabolites such as sclareol described here, since reconstruction of heterologous metabolic pathway often suffers from a mismatch between the tight regulation and the engineered pathway (Montano Lopez et al., 2022). To overcome this challenge, more elaborate design and genetic manipulation should be conducted for efficient biosynthesis. For example, our final sclareol overproducing strain contains 40 genetic manipulations (30 genes overexpression, 8 genes deletion and 2 promoter replacement). Reconstruction of a cell factory from scratch in wild-type backgrounds requires long time and multiple genetic manipulations. Here, we show that metabolic transforming at a modular manner facilitates the construction of versatile cell factories with saving 18 genetic manipulations, and the biosynthetic modules adapt well to the central metabolism. This metabolic transforming verified our principle that the platform cell factory is of great value to develop new cell factories relatively quickly (Nielsen, 2015; Nielsen and Keasling, 2016).

Millions of years of evolution have made primary metabolism a tightly regulated network, and resistant to flux alterations and/or to genetic modifications for over-production of target metabolites (Stephanopoulos and Vallino, 1991). Subtle engineering of metabolic networks failed to significantly alter the cellular phenotype (Gleizer et al., 2019) or improve the biosynthesis of a product of interest (Asadollahi et al., 2008; Nielsen and Keasling, 2016). Here, we showed that global metabolic rewiring improved the production of acetyl-CoA-derived molecules. Similarly, construction of an ethylene biosynthesis pathway with enhanced TCA cycle, enabled enhancing photosynthetic activity and redistributing metabolic flux for efficient production of ethylene from TCA cycle in cyanobacteria (Xiong et al., 2015).

Overall, we conclude global metabolic rewiring can shape new metabolic type, which can be adopted for overproduction of a variety of chemicals that are derived from other key node metabolites such as glucose 6-phosphate, pyruvate and malonyl-CoA.

Competing financial interests

Yongjin J. Zhou and Xuan Cao have filed a patent (PCT/CN2021/138,506) for protecting the production of sclareol in yeast. All other authors declare no conflicts of interest.

Author contributions

Xuan Cao: Methodology, investigation, formal analysis, validation, writing – original draft. Wei Yu: Methodology, investigation, writing – original draft. Yu Chen: Methodology. Shan Yang: Resources. Zongbao K. Zhao: Supervision. Jens Nielsen: Supervision. Hongwei Luan: Methodology. Yongjin J. Zhou: Funding acquisition, conceptualization, project administration, supervision, writing – review & editing.

Data availability

Data will be made available on request.

Acknowledgements

The authors acknowledge funding from National Natural Science Foundation of China (21922812 and 21877111), and Key project at central government level: The ability establishment of sustainable use for valuable Chinese medicine resources (2060302). The authors thank the Energy Biotechnology Platform of DICP for providing facility assistance. The authors thank AiMi Academic Services (www.aimieditor.com) for the English language editing.

Appendix A. Supplementary data

Supplementary data to this article can be found online at https://doi.org/10.1016/j.ymben.2022.11.002.

References

Ajikumar, P.K., Xiao, W.H., Tyo, K.E., Wang, Y., Simeon, F., Leonard, E., Mucha, O., Phon, T.H., Pfeifer, B., Stephanopoulos, G., 2010. Isoprenoid pathway optimization for Taxol precursor overproduction in *Escherichia coli*. Science 330 (6000), 70–74.

Asadollahi, M.A., Maury, J., Moller, K., Nielsen, K.F., Schalk, M., Clark, A., Nielsen, J., 2008. Production of plant sesquiterpenes in *Saccharomyces cerevisiae*: effect of ERG9 repression on sesquiterpene biosynthesis. Biotechnol. Bioeng. 99 (3), 666–677.

Callari, R., Meier, Y., Ravasio, D., Heider, H., 2018. Dynamic control of ERG20 and ERG9 expression for improved casbene production in *Saccharomyces cerevisiae*. Front. Bioeng. Biotechnol. 6, 160–170.

Chen, R., Yang, S., Zhang, L., Zhou, Y.J., 2020. Advanced strategies for production of natural products in yeast. iScience 23 (3), 100879.

Gaspar, M.E., Csermely, P., 2012. Rigidity and flexibility of biological networks. Briefings Funct. Genom. 11 (6), 443–456.

Geiselman, G.M., Zhuang, X., Kirby, J., Tran-Gyamfi, M.B., Prahl, J.P., Sundstrom, E.R., Gao, Y., Munoz Munoz, N., Nicora, C.D., Clay, D.M., Papa, G., Burnum-Johnson, K. E., Magnuson, J.K., Tanjore, D., Skerker, J.M., Gladden, J.M., 2020. Production of ent-kaurene from lignocellulosic hydrolysate in *Rhodosporidium toruloides*. Microb. Cell Factories 19 (1), 24–35.

Gleizer, S., Ben-Nissan, R., Bar-On, Y.M., Antonovsky, N., Noor, E., Zohar, Y., Jona, G., Krieger, E., Shamshoum, M., Bar-Even, A., Milo, R., 2019. Conversion of *Escherichia coli* to generate all biomass carbon from CO2. Cell 179 (6), 1255–1263.

Guo, X.Y., Liu, J.J., Zhang, C.B., Zhao, F.L., Lu, W.Y., 2019. Stepwise increase in the production of 13R-manoyl oxide through metabolic engineering of *Saccharomyces cerevisiae*. Biochem. Eng. J. 144, 73–80.

Heirendt, L., Arreckx, S., Pfau, T., 2019. Creation and analysis of biochemical constraint-based models using the COBRA Toolbox v.3.0. Nat. Protoc. 14 (3), 639–702.

Hu, T.Y., Zhou, J.W., Tong, Y.R., Su, P., Li, X.L., Liu, Y., Liu, N., Wu, X.Y., Zhang, Y.F., Wang, J.D., Gao, L.H., Tu, L.C., Lu, Y., Jiang, Z.Q., Zhou, Y.J.J., Gao, W., Huang, L. Q., 2020. Engineering chimeric diterpene synthases and isoprenoid biosynthetic pathways enables high-level production of miltiradiene in yeast. Metab. Eng. 60, 87–96.

Ignea, C., Trikka, F.A., Kourtzelis, I., Argiriou, A., Kanellis, A.K., Kampranis, S.C., Makris, A.M., 2012. Positive genetic interactors of *HMG2* identify a new set of genetic perturbations for improving sesquiterpene production in *Saccharomyces cerevisiae*. Microb. Cell Factories 11, 162–177.

Ignea, C., Trikka, F.A., Nikolaidis, A.K., Georgantea, P., Ioannou, E., Loupassaki, S., Kefalas, P., Kanellis, A.K., Roussis, V., Makris, A.M., Kampranis, S.C., 2015. Efficient diterpene production in yeast by engineering Erg20p into a geranylgeranyl diphosphate synthase. Metab. Eng. 27, 65–75.

Leonard, E., Ajikumar, P.K., Thayer, K., Xiao, W.H., Mo, J.D., Tidor, B., Stephanopoulos, G., Prather, K.L., 2010. Combining metabolic and protein engineering of a terpenoid biosynthetic pathway for overproduction and selectivity control. Proc. Natl. Acad. Sci. U. S. A. 107 (31), 13654–13659.

Lu, H., Li, F., Sánchez, B.J., Zhu, Z., Li, G., 2019. A consensus *S. cerevisiae* metabolic model Yeast8 and its ecosystem for comprehensively probing cellular metabolism. Nat. Commun. 10 (1), 3586.

Mans, R., van Rossum, H.M., Wijsman, M., Backx, A., Kuijpers, N.G., van den Broek, M., Daran-Lapujade, P., Pronk, J.T., van Maris, A.J., Daran, J.M., 2015. CRISPR/Cas9: a molecular Swiss army knife for simultaneous introduction of multiple genetic modifications in *Saccharomyces cerevisiae*. FEMS Yeast Res. 15 (2), fov004.

Meadows, A.L., Hawkins, K.M., Tsegaye, Y., Antipov, E., Kim, Y., Raetz, L., Dahl, R.H., Tai, A., Mahatdejkul-Meadows, T., Xu, L., Zhao, L., Dasika, M.S., Murarka, A., Lenihan, J., Eng, D., Leng, J.S., Liu, C.L., Wenger, J.W., Jiang, H., Chao, L., Westfall, P., Lai, J., Ganesan, S., Jackson, P., Mans, R., Platt, D., Reeves, C.D., Saija, P.R., Wichmann, G., Holmes, V.F., Benjamin, K., Hill, P.W., Gardner, T.S., Tsong, A.E., 2016. Rewriting yeast central carbon metabolism for industrial isoprenoid production. Nature 537 (7622), 694–697.

Megyeri, M., Prasad, R., Volpert, G., Sliwa-Gonzalez, A., Haribowo, A.G., Aguilera-Romero, A., Riezman, H., Barral, Y., Futerman, A.H., Schuldiner, M., 2019. Yeast ceramide synthases, Lag1 and Lac1, have distinct substrate specificity. J. Cell Sci. 132 (12), 228411–228419.

Meurisse, J., Bacquin, A., Richet, N., Charbonnier, J.B., Ochsenbein, F., Peyroche, A., 2014. Hug1 is an intrinsically disordered protein that inhibits ribonucleotide reductase activity by directly binding Rnr2 subunit. Nucleic Acids Res. 42 (21), 13174–13185.

Mikkelsen, M.D., Buron, L.D., Salomonsen, B., Olsen, C.E., Hansen, B.G., Mortensen, U. H., Halkier, B.A., 2012. Microbial production of indolic glucosinolate through engineering of a multi-gene pathway in a versatile yeast expression platform. Metab. Eng. 14 (2), 104–111.

Montano Lopez, J., Duran, L., Avalos, J.L., 2022. Physiological limitations and opportunities in microbial metabolic engineering. Nat. Rev. Microbiol. 20 (1), 35–48.

Nielsen, J., 2015. Yeast cell factories on the horizon. Science 349 (6252), 1050–1051.

Nielsen, J., Keasling, J.D., 2016. Engineering cellular metabolism. Cell 164 (6), 1185–1197.
Nowrouzi, B., Li, R.A., Walls, L.E., d'Espaux, L., Malci, K., Liang, L., Jonguitud-Borrego, N., Lerma-Escalera, A.I., Morones-Ramirez, J.R., Keasling, J.D., Rios-Solis, L., 2020. Enhanced production of taxadiene in *Saccharomyces cerevisiae*. Microb. Cell Factories 19 (1), 200.
Odat, O., Matta, S., Khalil, H., Kampranis, S.C., Pfau, R., Tsichlis, P.N., Makris, A.M., 2007. Old yellow enzymes, highly homologous FMN oxidoreductases with modulating roles in oxidative stress and programmed cell death in yeast. J. Biol. Chem. 282 (49), 36010–36023.
Polakowski, T., Stahl, U., Lang, C., 1998. Overexpression of a cytosolic hydroxymethylglutaryl-CoA reductase leads to squalene accumulation in yeast. Appl. Microbiol. Biotechnol. 49 (1), 66–71.
Reider Apel, A., d'Espaux, L., Wehrs, M., Sachs, D., Li, R.A., Tong, G.J., Garber, M., Nnadi, O., Zhuang, W., Hillson, N.J., Keasling, J.D., Mukhopadhyay, A., 2017. A Cas9-based toolkit to program gene expression in *Saccharomyces cerevisiae*. Nucleic Acids Res. 45 (1), 496–508.
Schalk, M., Pastore, L., Mirata, M.A., Khim, S., Schouwey, M., Deguerry, F., Pineda, V., Rocci, L., Daviet, L., 2012. Toward a biosynthetic route to sclareol and amber odorants. J. Am. Chem. Soc. 134 (46), 18900–18903.
Stephanopoulos, G., Vallino, J.J., 1991. Network rigidity and metabolic engineering in metabolite overproduction. Science 252 (5013), 1675–1681.
Tokuhiro, K., Muramatsu, M., Ohto, C., Kawaguchi, T., Obata, S., Muramoto, N., Hirai, M., Takahashi, H., Kondo, A., Sakuradani, E., Shimizu, S., 2009. Overproduction of geranylgeraniol by metabolically engineered *Saccharomyces cerevisiae*. Appl. Environ. Microbiol. 75 (17), 5536–5543.
Trikka, F.A., Nikolaidis, A., Athanasakoglou, A., Andreadelli, A., Ignea, C., Kotta, K., Argiriou, A., Kampranis, S.C., Makris, A.M., 2015. Iterative carotenogenic screens identify combinations of yeast gene deletions that enhance sclareol production. Microb. Cell Factories 14, 60.
Verduyn, C., Postma, E., Scheffers, W.A., Van Dijken, J.P., 1992. Effect of benzoic acid on metabolic fluxes in yeasts: a continuous-culture study on the regulation of respiration and alcoholic fermentation. Yeast 8 (7), 501–517.
Wu, G., Yan, Q., Jones, J.A., Tang, Y.J., Fong, S.S., Koffas, M.A.G., 2016. Metabolic burden: cornerstones in synthetic biology and metabolic engineering applications. Trends Biotechnol. 34 (8), 652–664.
Xie, W., Ye, L., Lv, X., Xu, H., Yu, H., 2015. Sequential control of biosynthetic pathways for balanced utilization of metabolic intermediates in *Saccharomyces cerevisiae*. Metab. Eng. 28, 8–18.
Xiong, W., Morgan, J.A., Ungerer, J., Wang, B., Maness, P.C., Yu, J.P., 2015. The plasticity of cyanobacterial metabolism supports direct CO2 conversion to ethylene. Nat. Plants 1 (5), 15085–15090.
Yang, S., Cao, X., Yu, W., Li, S., Zhou, Y.J., 2020. Efficient targeted mutation of genomic essential genes in yeast *Saccharomyces cerevisiae*. Appl. Microbiol. Biotechnol. 104 (7), 3037–3047.
Yang, W., Zhou, Y., Liu, W., Shen, H., Zhao, Z.K., 2013. Engineering *Saccharomyces cerevisiae* for sclareol production. Sheng Wu Gong Cheng Xue Bao 29 (8), 1185–1192.
Yu, T., Zhou, Y.J., Huang, M., Liu, Q., Pereira, R., David, F., Nielsen, J., 2018. Reprogramming yeast metabolism from alcoholic fermentation to lipogenesis. Cell 174 (6), 1549–1558 e14.
Zerbe, P., Bohlmann, J., 2015. Enzymes for synthetic biology of ambroxide-related diterpenoid fragrance compounds. Adv. Biochem. Eng. Biotechnol. 148, 427–447.
Zhang, C., Ju, H., Lu, C.Z., Zhao, F., Liu, J., Guo, X., Wu, Y., Zhao, G.R., Lu, W., 2019. High-titer production of 13R-manoyl oxide in metabolically engineered *Saccharomyces cerevisiae*. Microb. Cell Factories 18 (1), 73.
Zhou, Y.J., Buijs, N.A., Zhu, Z., Qin, J., Siewers, V., Nielsen, J., 2016. Production of fatty acid-derived oleochemicals and biofuels by synthetic yeast cell factories. Nat. Commun. 7, 11709.
Zhou, Y.J., Gao, W., Rong, Q., Jin, G., Chu, H., Liu, W., Yang, W., Zhu, Z., Li, G., Zhu, G., Huang, L., Zhao, Z.K., 2012. Modular pathway engineering of diterpenoid synthases and the mevalonic acid pathway for miltiradiene production. J. Am. Chem. Soc. 134 (6), 3234–3241.
Zhou, Y.J., 2018. Expanding the terpenoid kingdom. Nat. Chem. Biol. 14 (12), 1069–1070.